

Microscopic description of fission in nobelium isotopes with the Gogny-D1M energy density functional

R. Rodríguez-Guzmán

Physics Department, Kuwait University, Kuwait 13060, Kuwait

L.M. Robledo

Departamento de Física Teórica, Universidad Autónoma de Madrid, 28049-Madrid, Spain

(Dated: December 2, 2016)

Constrained mean-field calculations, based on the Gogny-D1M energy density functional, have been carried out to describe fission in the isotopes $^{250-260}\text{No}$. The even-even isotopes have been considered within the standard Hartree-Fock-Bogoliobov (HFB) framework while for the odd-mass ones the Equal Filling Approximation (HFB-EFA) has been employed. Ground state quantum numbers and deformations, pairing energies, one-neutron separation energies, inner and outer barrier heights as well as fission isomer excitation energies are given. Fission paths, collective masses and zero-point quantum vibrational and rotational corrections are used to compute the systematic of the spontaneous fission half-lives t_{SF} both for even-even and odd-mass nuclei. Though there exists a strong variance of the predicted fission rates with respect to the details involved in their computation, it is shown that both the specialization energy and the pairing quenching effects, taken into account within the self-consistent HFB-EFA blocking procedure, lead to larger t_{SF} values in odd-mass nuclei as compared with their even-even neighbors. Alpha decay lifetimes have also been computed using a parametrization of the Viola-Seaborg formula. The high quality of the Gogny-D1M functional regarding nuclear masses leads to a very good reproduction of Q_α values and consequently of lifetimes.

PACS numbers: 24.75.+i, 25.85.Ca, 21.60.Jz, 27.90.+b, 21.10.Pc

I. INTRODUCTION

The theoretical description of odd-mass nuclei still remains as a major challenge in nuclear structure as compared to the treatment of even-even nuclei. Nevertheless, odd-mass nuclei provide key information regarding not only odd-even effects associated to pairing correlations but also the “time-odd” section of the nuclear energy density functional (EDF) which is of paramount relevance in the dynamical behavior of the nucleus. In addition, odd-mass nuclei could also be useful to constrain the parameters of energy density functionals (EDFs) with the aim to reach a reasonable spectroscopic quality. Moreover, the energies, spins and parities of their low-lying one-quasiparticle spectra provide insight into the underlying shell effects. Thus, the properties of odd-mass nuclei and the computational challenge in their evaluation have received renewed attention in recent years (see, for example, [1–11] and references therein).

In the context of spontaneous fission [12–14], it is experimentally observed that the half-lives t_{SF} of odd-mass nuclei are systematically larger than the ones of their even-even neighbors. Two complementary mechanisms have been proposed to explain this feature: One is the specialization energy [15], that modifies the collective potential energy landscape felt by the odd-mass nucleus in its evolution from the ground state to scission as compared to the one of the neighboring even-even companions. The origin of part of this energy is the assumption that the K quantum number associated with the projection of the angular momentum onto the intrinsic sym-

metry axis characteristic of any odd-mass quantum state has to be conserved along the fission process. The reason behind this assumption is that the time scale for fission (not to be confused with the t_{SF} value) is of the order of the one for the strong interaction and, therefore, much shorter than the typical time scales for the electromagnetic processes responsible for the change of the K quantum number. The second mechanism is the characteristic quenching of pairing correlations caused by the unpaired nucleon that weakens the pairing field strengths, as compared with the fully paired situation, enhancing the collective inertia that strongly depends on the pairing gap. This enhancement in turn, increases the collective action and, therefore, the spontaneous fission half-life t_{SF} . One should also keep in mind, that fission observables are quite sensitive to pairing correlations owing to the strong dependence of the collective inertias on the inverse of the square of the pairing gap [16–21].

Within the EDF framework, it is customary to describe the transition from a single even-even system to its fragments in terms of several deformation parameters [12, 13, 22–24]. Such microscopic (constrained) EDF calculations already represent a highly demanding computational task. They are usually carried out using mean-field approximations based on nonrelativistic Gogny [19–21, 25–31], Skyrme [23, 24, 32–36] and more recently Barcelona-Catania-Paris-Madrid (BCPM) [16, 37] as well as relativistic [38–42] EDFs. What further complicates the EDF description of fission in odd-mass nuclei is the need to consider, for each intrinsic configuration along the fission path, blocked one-quasiparticle

wave functions [43]. The blocked wave functions break time-reversal invariance which requires the evaluation of time-odd fields. Typically, this requirement represents a factor of two more computing time in the solution of the Hartree-Fock-Bogoliubov (HFB) equations as compared to the even-even case where the time-odd fields are zero by construction. On the other hand, due to the (non-linear) self-consistent character of the HFB equations, there is no guarantee to obtain the lowest energy solution by blocking the quasiparticle with the lowest one-quasiparticle excitation energy. Therefore, the blocking procedure has to be repeated for several low-lying one-quasiparticle states.

From what has already been mentioned above, it is clear that an approximation is required in order to afford the computational cost of the microscopic EDF description of fission in odd-mass nuclei. Within this context, the Equal Filling Approximation (EFA) represents a reasonable starting point still preserving time-reversal invariance [2, 3, 5–8, 44]. The EFA has been proven to be a fully variational method by recasting it in terms of the language of quantum statistical mechanics and the introduction of a statistical ensemble where one-quasiparticle configurations and their time-reversed companions are present with equal probability [2]. One advantage of this point of view is that the results of finite temperature HFB and its extensions to compute collective inertias in the framework of the Adiabatic Time Dependent (ATD) method [45–47] can be used to compute the collective inertias needed to obtain the t_{SF} values for odd-mass nuclei.

Nuclei in the No ($Z=102$) region have attracted considerable attention [11] thanks to the progress made in the production of super-heavy elements (see, for example, [48] and references therein) but also because of the rich spectroscopic data obtained for them [49]. In this paper, we mainly focus on the HFB-EFA description of the fission properties in odd-mass nobelium isotopes. To the best of our knowledge our EDF calculations are the first of their kind reported in the literature. For the sake of completeness, we also discuss results for even-even No nuclei. We have studied the sample of nuclei $^{250-260}\text{No}$. The odd-mass isotopes are considered within the (constrained) HFB-EFA [2, 3, 5–8, 44] while for the even-even ones calculations have been carried out using the standard (constrained) HFB framework [19–21, 43].

Our HFB and/or HFB-EFA calculations are based on the parametrization D1M [50] of the Gogny-EDF [51]. In previous studies [19–21], we have performed fission calculations for neutron-rich Ra, U and Pu nuclei as well as for a sample of heavy and super-heavy nuclei for which experimental data exist. The comparison between the D1S [25], D1N [52] and D1M [50] Gogny-EDFs, with available experimental data and other theoretical results, reveals that the parameter set D1M represents a reasonable starting point to describe fission in heavy and super-heavy nuclei. This is quite satisfying as the Gogny-D1M EDF does a much better job to reproduce nuclear

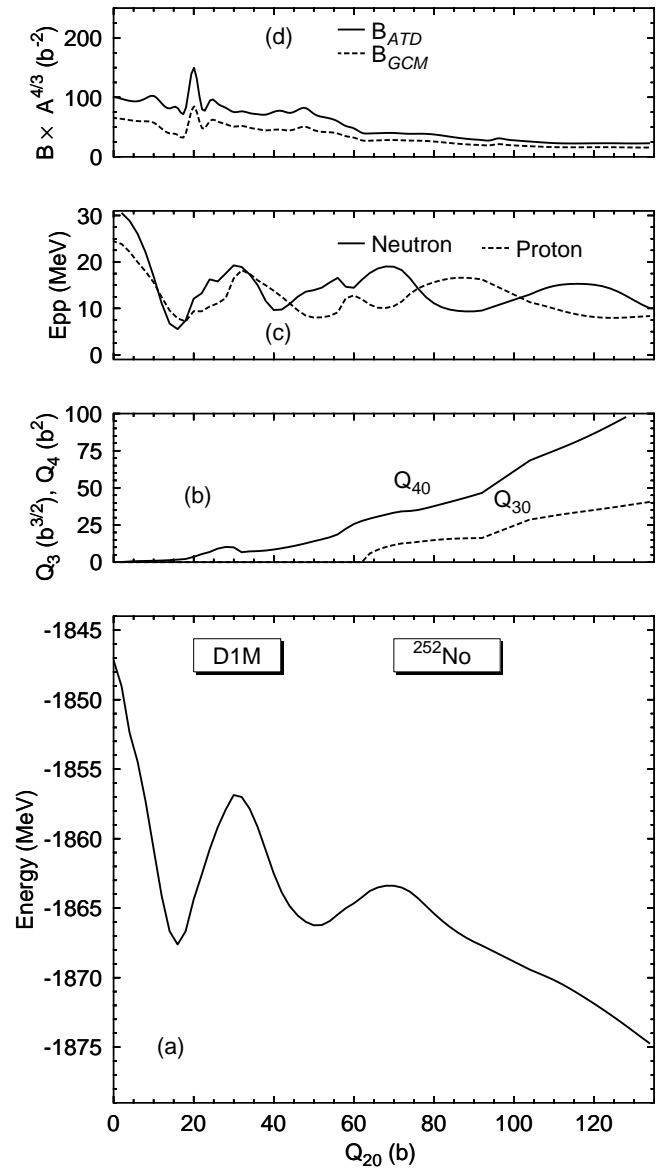


FIG. 1: The HFB plus the zero-point rotational energies, are plotted in panel (a) as functions of the quadrupole moment Q_{20} for the nucleus ^{252}No . The octupole Q_{30} and hexadecupole Q_{40} moments are given in panel (b). The pairing interaction energy $E_{pp} = 1/2\text{Tr}\Delta\kappa^*$ is depicted in panel (c) for protons (dashed lines) and neutrons (full lines). The collective GCM (dashed lines) and ATD (full lines) masses are plotted in panel (d). For more details, see the main text.

masses [50] and, at the same time, seems to keep essentially the same predictive power of the well tested D1S parametrization [7, 8, 50, 53–56] to reproduce low-energy nuclear structure data. However, more work is needed in order to substantiate this conclusion, especially in the case of fission where the D1M parametrization has been scarcely used. In particular, in this study we explore, for the first time, the ability of the Gogny-D1M EDF framework to capture basic fission properties along the No isotopic chain including not only even-even but also

odd-mass nuclei.

The paper is organized as follows. In Sec. II, we briefly outline the HFB-EFA [2, 5–8, 44]. For details on the HFB framework for even-even nuclei the reader is referred to [19–21, 43]. The results of our calculations are presented in Sec. III where we discuss the fission paths, ground state quantum numbers and deformations, first and second barrier heights, fission isomers, spontaneous fission and α -decay half-lives for $^{250-260}\text{No}$ and compare, whenever possible, with the available experimental data [57, 58]. In particular, we illustrate our methodology for both ^{252}No and ^{253}No in Secs. III A and III B while the systematic of the fission paths and spontaneous fission half-lives in $^{250-260}\text{No}$ is presented in Secs. III C and III D. Let us stress that in this study, we implicitly assume that the properties of the considered No isotopes are determined by general features of the Gogny-D1M EDF and therefore, no fine tuning of its parameters has been done. Finally, Sec. IV is devoted to the concluding remarks and work perspectives.

II. THEORETICAL FRAMEWORK

In this section, we briefly outline the (constrained) HFB-EFA [2, 5–8, 44] used to compute the fission paths for $^{251,253,255,257,259}\text{No}$. Calculations for $^{250,252,254,256,258,260}\text{No}$ have been carried out within the (constrained) HFB approach and, for details, the reader is referred to [19–21, 43].

The description of odd-mass systems requires, blocked (product) one-quasiparticle wave functions $|\Psi_\mu\rangle = \hat{\alpha}_\mu^\dagger |\Psi\rangle$, which are given in terms of a fully paired reference vacuum $|\Psi\rangle$ and the quasiparticle creator [43] $\hat{\alpha}_\mu^\dagger$ for the state μ to be blocked. The states $|\Psi_\mu\rangle$, as well as their density matrix and pairing tensor break the time-reversal invariance and so do the Hartree-Fock and pairing fields [43] associated with them. Furthermore, the density matrix and pairing tensor are no longer invariant under unitary transformations of the Bogoliubov amplitudes U and V [43] applied to the right and therefore, reorientation effects [9, 10] should also be taken into account in the solution of the mean-field equations. Therefore, in order to alleviate the numerical effort, we have resorted to the HFB-EFA within which one considers the following density matrix

$$\begin{aligned} \rho_{ij}^{(\mu,EFA)} &= \frac{1}{2} \left(\langle \Psi_\mu | \hat{c}_j^\dagger \hat{c}_i | \Psi_\mu \rangle + \langle \Psi_{\bar{\mu}} | \hat{c}_j^\dagger \hat{c}_i | \Psi_{\bar{\mu}} \rangle \right) \\ &= (V^* V^T)_{ij} + \frac{1}{2} (U_{i\mu} U_{j\bar{\mu}}^* - V_{i\mu}^* V_{j\bar{\mu}}) \\ &\quad + \frac{1}{2} (U_{i\bar{\mu}} U_{j\mu}^* - V_{i\bar{\mu}}^* V_{j\mu}) \end{aligned} \quad (1)$$

and pairing tensor

$$\kappa_{ij}^{(\mu,EFA)} = \frac{1}{2} (\langle \Psi_\mu | \hat{c}_j \hat{c}_i | \Psi_\mu \rangle + \langle \Psi_{\bar{\mu}} | \hat{c}_j \hat{c}_i | \Psi_{\bar{\mu}} \rangle)$$

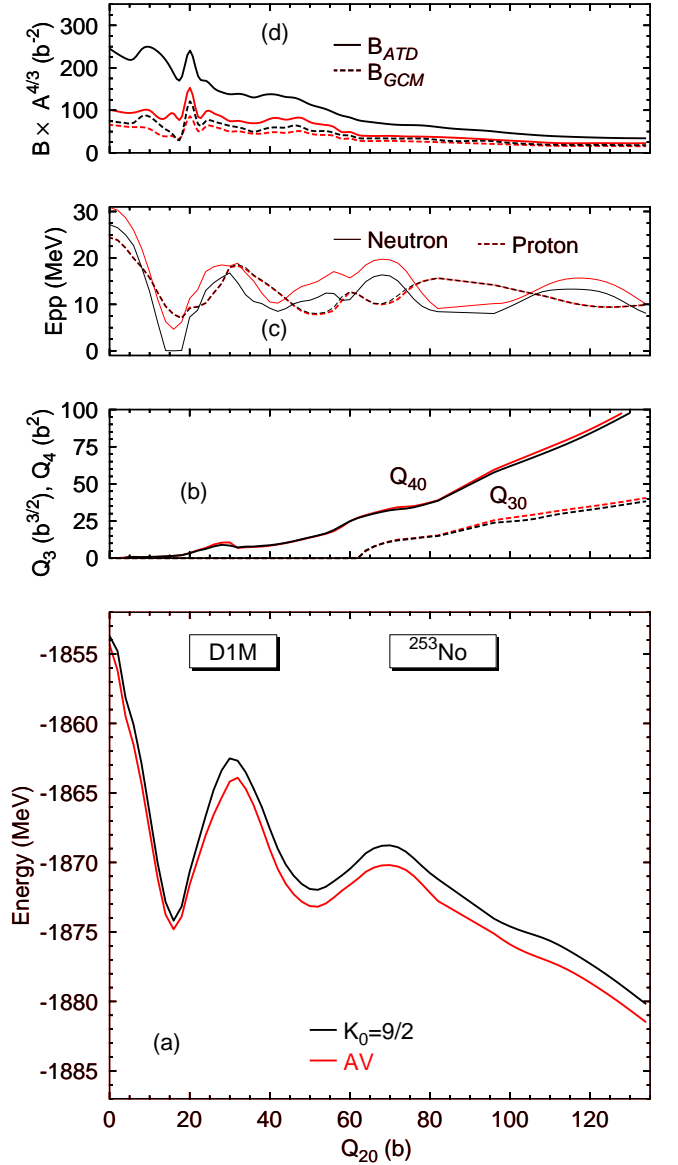


FIG. 2: (Color online) The $K_0 = 9/2$ HFB-EFA plus the zero-point rotational energies, are plotted in panel (a) as functions of the quadrupole moment Q_{20} for the nucleus ^{253}No . The octupole Q_{30} and hexadecupole Q_{40} moments are given in panel (b). The pairing interaction energies are depicted in panel (c) for protons (dashed lines) and neutrons (full lines). The collective GCM (dashed lines) and ATD (full lines) masses are plotted in panel (d). Results corresponding to "average" (AV) HFB calculations for ^{253}No have also been included in each panel (red). For more details, see the main text.

$$\begin{aligned} &= (V^* U^T)_{ij} + \frac{1}{2} (U_{i\mu} V_{j\bar{\mu}}^* - V_{i\mu}^* U_{j\bar{\mu}}) \\ &\quad + \frac{1}{2} (U_{i\bar{\mu}} V_{j\mu}^* - V_{i\bar{\mu}}^* U_{j\mu}) \end{aligned} \quad (2)$$

Intuitively, $\rho_{ij}^{(\mu,EFA)}$ and $\kappa_{ij}^{(\mu,EFA)}$ correspond to an occupancy of $1/2$ for the quasiparticle state μ and its Kramers' partner $\bar{\mu}$, thus preserving time-reversal invari-

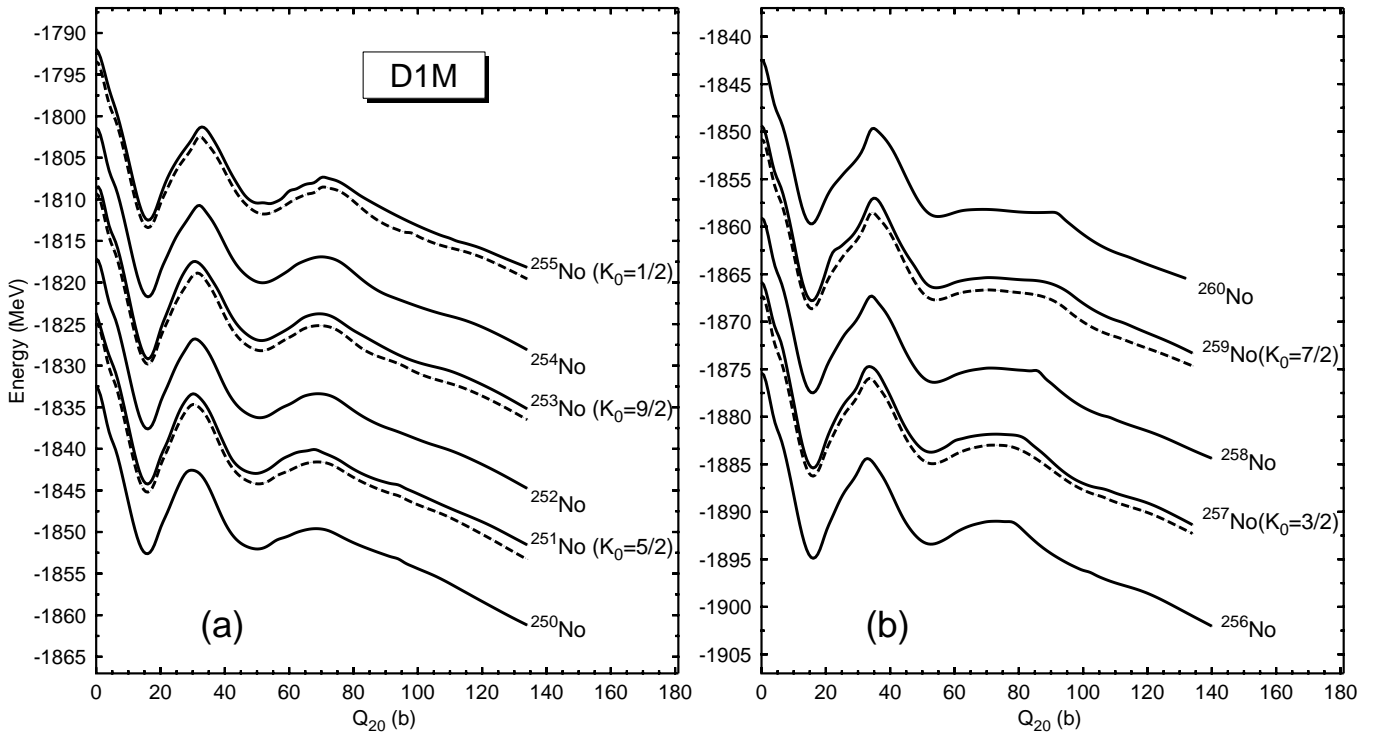


FIG. 3: The ground state fission paths obtained for the isotopes $^{250-260}\text{No}$ are plotted as functions of the quadrupole moment Q_{20} . Starting from the nucleus ^{251}No (^{257}No) in panel (a) [panel (b)], the curves have been shifted by 15 MeV in order to accommodate them in a single plot. For $^{251,253,255,257,259}\text{No}$, the corresponding K_0 values are included in the plot. The "average" (AV) fission paths for those odd-mass nuclei are also depicted with dashed lines. For more details, see the main text.

ance. This intuition can be substantiated by proving the existence of a statistical density matrix operator [2] that produces exactly the same density matrix and pairing tensor. The help of Gaudin's theorem [59, 60] is required to compute all the basic contractions in Eqs. (1) and (2), as well as the mean values of any kind of operator within the HFB-EFA. The total HFB-EFA energy, which is the statistical average of the EDF with the special statistical density described above, can then be written in the usual form in terms of $\rho_{ij}^{(\mu,EFA)}$ and $\kappa_{ij}^{(\mu,EFA)}$ [43]. The Ritz-variational principle applied to the HFB-EFA energy leads to the HFB-EFA equations that can be solved using the standard gradient method [61], with the subsequent simplification in the treatment of several constraints [2, 5–8].

Let us now turn our attention to the practical aspects of the methodology employed in this work to obtain the ground state fission path in the case of ^{253}No (see, Sec. III B) taken, as an illustrative example. The same methodology has been used for all the studied odd-mass No isotopes.

Step 1) We have computed the fission path for ^{252}No (see, Sec. III A) using the HFB approach with constraints on the axially symmetric quadrupole \hat{Q}_{20} and octupole \hat{Q}_{30} operators [53, 54]. Here, as well as in Steps 2, 3 and 4 below, we have imposed an additional constraint on the operator \hat{Q}_{10} , to avoid spurious center-of-mass

effects. We have used a deformed axially symmetric harmonic oscillator (HO) basis consisting of states with J_z quantum numbers up to $35/2$ and up to 26 quanta in the z -direction [19]. The oscillator lengths b_z and b_\perp for each value of $Q_{20} = \langle \hat{Q}_{20} \rangle$ have been optimized as to minimize the energy. Zero-point quantum rotational ΔE_{ROT} and vibrational ΔE_{vib} energies have been added *a posteriori* to the HFB energies [19–21].

Step 2) Using the HFB states (Step 1) as initial wave functions in the iterative mean-field procedure, we have computed an "average" (AV) fission path for ^{253}No (see, Fig. 2). In order to obtain the AV HFB states, calculations have been carried out as for an even-even nucleus but with a constraint on the mean value of the neutron number operator to be $\langle \hat{N} \rangle = 151$. We have used the single-particle basis with the (optimized) HO lengths b_z and b_\perp resulting from Step 1. Zero-point quantum corrections have also been added to the mean-field energies [19–21].

Step 3) Using the HFB wave function corresponding to the absolute (normal deformed) minimum of the AV path (Step 2) in ^{253}No as starting state, we have performed a set of HFB-EFA blocking calculations to identify the $K=K_0$ value corresponding to the ground state. To this end, we have repeated the blocking procedure several times, using the same single-particle basis as in Step 2. We have obtained three different solutions of

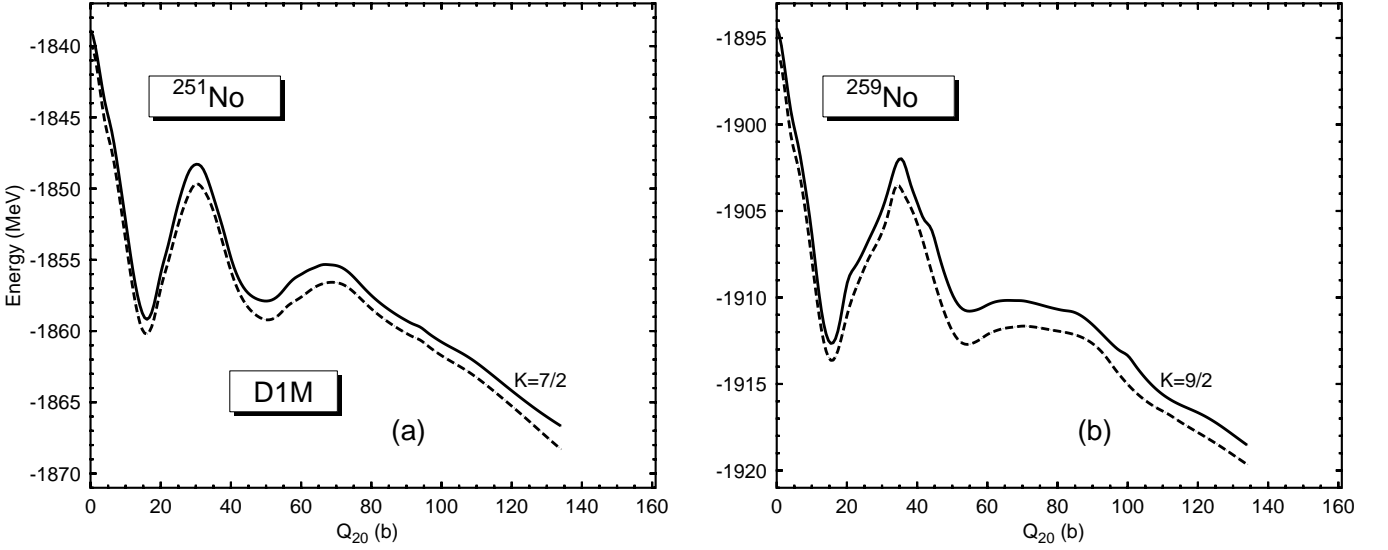


FIG. 4: The $K = 7/2$ and $9/2$ fission paths obtained for the isotopes ^{251}No and ^{259}No are plotted as functions of the quadrupole moment Q_{20} in panels (a) and (b), respectively. The "average" (AV) fission paths are also depicted with dashed lines. For more details, see the main text.

the HFB-EFA equations for each of the K values from $K=1/2$ up to $11/2$. Larger K values have not been taken into account as the neutron single-particle levels corresponding to them are too far from the Fermi surfaces. In addition to K_0 , the ground states obtained for all the odd-mass isotopes studied in this work are characterized by their parity π . We will refer to them hereafter, as K_0^π configurations.

Step 4) Using the AV HFB states (Step 2) as starting wave functions, we have computed the K_0 (i.e., ground state) fission path for ^{253}No . Note that we are assuming that for an odd-mass nucleus with the ground state quantum numbers K_0^π , the spontaneous fission will take place in a configuration with the same K_0 (parity can be broken in the fission process). For each (Q_{20}, Q_{30}) -configuration, we have considered the blocking of several quasiparticle states so as to obtain three different K_0 -solutions of the HFB-EFA equations. From these three K_0 -solutions, the one with the lowest energy is used to build the ground state fission path for ^{253}No . In this step we use the same single-particle basis as in Step 2 and with the same oscillator lengths.

Let us mention, that in our Gogny-D1M mean-field calculations (Steps 1 to 4) the two-body kinetic energy correction has been fully taken into account in the Ritz-variational procedure while for the Coulomb exchange term we have considered the Slater approximation. The spin-orbit contribution to the pairing field has been neglected.

The computational cost to produce a plain potential energy surface requiring 75 constrained HFB calculations is of the order of five hours in a modern personal computer. If the oscillator lengths have to be optimized at each Q_{20} value then the cost is a factor of 5 higher (Step 1). The computational cost of the EFA is in principle

similar to the one of HFB as time odd-fields are not considered. However, in the EFA case several initial blocked configurations (three in our case) have to be considered. In addition, the number of iteration required to solve the EFA problem is typically two or three times larger than the one to solve HFB and therefore the typical cost of an EFA calculation is ten times higher than the one of a HFB calculation.

For the rotational correction to the HFB-EFA energies, we have taken the expression $\Delta E_{\text{ROT}} = \langle \Delta \hat{J}^2 \rangle / 2\mathcal{T}_Y$. However, both $\langle \Delta \hat{J}^2 \rangle$ and the Yoccoz \mathcal{T}_Y moment of inertia have been computed using the formulas for even-even nuclei [62–64]. The reason is that an approximate angular momentum projection has not yet been carried out within the HFB-EFA framework. Work along these lines is in progress and will be reported elsewhere. On the other hand, the Adiabatic Time Dependent HFB (ATDHF) framework has already been developed in the realm of quantum statistical mechanics [45–47] allowing its verbatim extension to the HFB-EFA via its statistical density matrix operator [2]. In particular, the ATD vibrational energy correction reads

$$\Delta E_{\text{vib}, \text{ATD}} = \frac{1}{4} \frac{\mathcal{M}_{-2}}{\mathcal{M}_{-1}^2} B_{\text{ATD}}^{-1} \quad (3)$$

For the evaluation of the collective mass B_{ATD} in Eq. (3), we have resorted to the cranking approximation [65–68]. In this case

$$B_{\text{ATD}} = \frac{1}{2} \frac{\mathcal{M}_{-3}}{\mathcal{M}_{-1}^2} \quad (4)$$

with moments

$$(\mathcal{M}_{-n})_{ij} = \sum_{\mu\nu} \frac{Q_{i\mu\nu} Q_{j\nu\mu}}{(\bar{\mathcal{E}}_\mu - \bar{\mathcal{E}}_\nu)^n} (\bar{\rho}_\mu - \bar{\rho}_\nu) \quad (5)$$

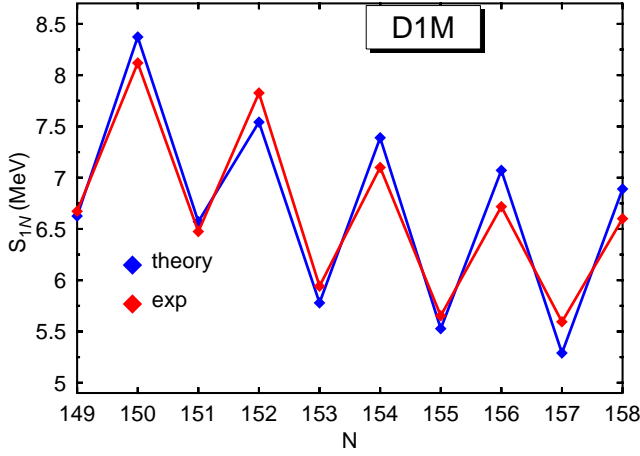


FIG. 5: (Color online) The one-neutron S_{1N} separation energies are plotted as functions of the neutron number. Experimental values are taken from [58].

and

$$\mathcal{Q}_i = \begin{pmatrix} Q_i^{11} & Q_i^{20} \\ -Q_i^{20*} & -Q_i^{11*} \end{pmatrix} \quad (6)$$

In Eq. (6), Q_i^{11} and Q_i^{20} are the 11 and 20-components of the considered operator in the quasiparticle representation [43]. The matrix $\bar{\rho}$ takes the form

$$\bar{\rho} = \begin{pmatrix} f & 0 \\ 0 & 1 - f \end{pmatrix} \quad (7)$$

where the f 's are the quasiparticle HFB-EFA occupation factors (1/2 for the μ and $\bar{\mu}$ levels, respectively) while

$$\bar{\mathcal{E}} = \begin{pmatrix} E & 0 \\ 0 & -E \end{pmatrix} \quad (8)$$

where E_μ represents the quasiparticle energy.

In the case of even-even nuclei, one usually considers the GCM collective masses in addition to the ATD ones [19–21]. Though the use of the former in the case of odd-mass systems lacks the theoretical justification available for the latter within the HFB-EFA, we have also considered their phenomenology in the present study in order to examine the impact of such a prescription on the computed t_{SF} values. To this end, for the collective GCM masses in odd-mass No isotopes we have adopted the expression

$$B_{GCM} = \frac{1}{2} \frac{\mathcal{M}_{-2}^2}{\mathcal{M}_{-1}^3} \quad (9)$$

and $E_{\text{vib,GCM}}$ is given by Eq. (3) but replacing the ATD mass with the GCM one. The moments \mathcal{M}_{-n} are given by Eq. (5). For a thorough comparison of different forms of the collective masses in the framework of the Skyrme-EDF approximation, the reader is referred to [69].

As a consequence of the cranking approximation, which essentially amounts to neglecting the residual interaction in the evaluation of collective masses, divergences might appear in the computation of the moments Eq. (5) due to level crossings in the denominator. A phenomenological way to deal with the problem is to replace those denominators by $\sqrt{(E_\mu - E_\nu)^2 + \delta^2}$, with δ being a regularization factor introduced to simulate the effect of the residual interaction [70].

With all the required quantities at hand, we have computed the spontaneous fission half-life t_{SF} for the studied odd-mass nuclei using both the ATD and GCM schemes for the collective masses and zero-point vibrational corrections. For details regarding even-even isotopes the reader is referred to [19–21]. Within the Wentzel-Kramers-Brillouin (WKB) formalism [69, 71] the t_{SF} value (in seconds) is given by

$$t_{SF} = 2.86 \times 10^{-21} \times (1 + e^{2S}) \quad (10)$$

where the action S along the (minimal energy, one-dimensional projected) fission path reads

$$S = \int_a^b dQ_{20} \sqrt{2B(Q_{20}) [V(Q_{20}) - (E_{GS} + E_0)]}. \quad (11)$$

In this expression, the integration limits a and b are the classical turning points [17] below the barrier corresponding to the energy $E_{GS} + E_0$. The collective potential $V(Q_{20})$ is given by the HFB-EFA energy corrected by the zero-point rotational $\Delta E_{\text{ROT}}(Q_{20})$ and vibrational $\Delta E_{\text{vib}}(Q_{20})$ energies. The parameter E_0 accounts for the true ground state energy once the zero-point quadrupole fluctuations are considered. Although it is not difficult to estimate its value using the curvature of the energy around the ground state minimum and the values of the collective inertias [35] we have followed the usual recipe [16, 29] of considering it as a free parameter that takes four different values (i.e., $E_0 = 0.5, 1.0, 1.5$ and 2.0 MeV). In this way we can estimate its impact on the predicted spontaneous fission half-lives. Note, that different E_0 values provide different classical turning points a and b in Eq. (11) and therefore modify the final value of the action integral. As in previous studies [19–21], we have overlooked the E_0 -dependence of the pre-factor in front of the exponential of the action in Eq. (10) due to the large uncertainties in the estimation of the spontaneous fission half-lives arising from other sources.

Finally, we have computed the α -decay half-lives t_α using the Viola-Seaborg formula [75]

$$\log_{10} t_\alpha = \frac{AZ + B}{\sqrt{Q_\alpha}} + CZ + D + h_{\log} \quad (12)$$

with the parameters A, B, C, D and h_{\log} given in [74]. The Q_α value is obtained from the calculated binding energies for No and Fm nuclei.

III. DISCUSSION OF THE RESULTS

In this section we discuss the results of our Gogny-D1M calculations. First, in Secs. III A and III B, we consider the nuclei ^{252}No and ^{253}No as illustrative outcomes of our calculations. A similar analysis, as described below, has been carried out for all the studied even-even and odd-mass No isotopes. The systematic of the fission paths and spontaneous fission half-lives in $^{250-260}\text{No}$ is presented in Secs. III C and III D, respectively.

A. The nucleus ^{252}No

The HFB plus the zero-point rotational energies, are plotted in panel (a) of Fig. 1 as functions of the quadrupole moment for ^{252}No . The zero point vibrational energies are not included in the plot, as they are rather constant as functions of Q_{20} . However, they are always included in the computation of the spontaneous fission and α -decay half-lives. The octupole Q_{30} and hexadecupole Q_{40} moments are given in panel (b). The ground state for ^{252}No is located at $Q_{20} = 16$ b and is reflection symmetric. The fission isomer at $Q_{20} = 52$ b lies 1.38 MeV above the ground state from which, it is separated by the inner barrier ($Q_{20} = 30$ b) with the height of 10.75 MeV. As in the ground state case, the fission isomer is also reflection symmetric, a property that is shared for all the configurations belonging to the first barrier. However, as deduced from panel (b), octupole correlations play a role for quadrupole deformations $Q_{20} \geq 62$ b. Those correlations significantly affect the outer barrier ($Q_{20} = 70$ b) whose height is 4.23 MeV.

The proton and neutron pairing interaction energies $E_{pp} = 1/2\text{Tr}(\Delta\kappa^*)$ are depicted in panel (c). The neutron E_{pp} values exhibit minima (maxima) at $Q_{20} = 16, 40$ and 88 b (30, 68 and 120 b) while for protons those minima (maxima) correspond to $Q_{20} = 18, 50$ and 68 b (30, 60 and 88 b). The minima of E_{pp} are related to the minima of the potential energy surface (PES), a fact that can be understood in terms of level densities: minima of the PES correspond to low level density regions (Jahn-Teller effect) and the amount of pairing correlations is proportional to the level density around the Fermi level. On the other hand, maxima of the PES are associated to high level density regions implying stronger pairing correlations.

The collective GCM and ATD masses are plotted in panel (d). Their behavior is well correlated with the one of the pairing correlations in panel (c) and the inverse dependence of the collective mass with the square of the pairing gap [17, 18]. We also observe that the ATD masses are systematically larger than the GCM ones. For example, for $Q_{20} = 20$ b we have obtained the ratio $B_{\text{ATD}}/B_{\text{GCM}} = 1.77$. Such differences can have a strong impact on the predicted fission half-lives [16, 19–21] and are the reason why both kinds of collective masses have been considered in the computation of the t_{SF} values.

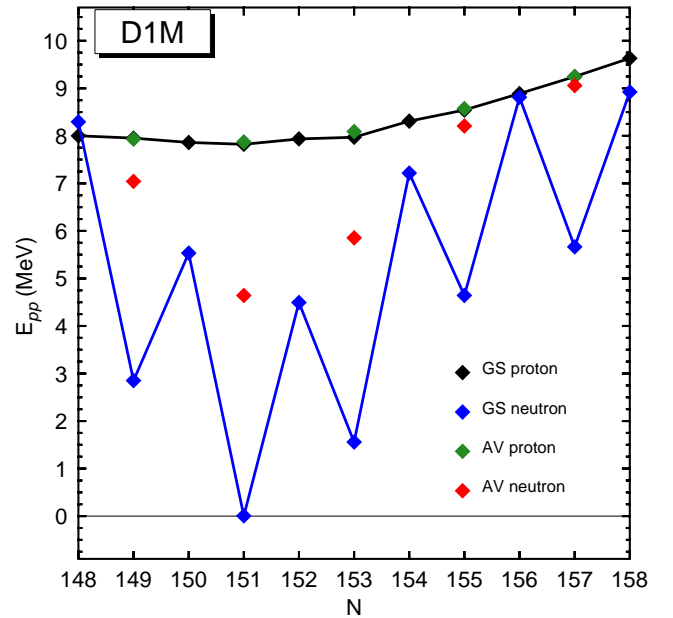


FIG. 6: (Color online) The proton and neutron pairing interaction energies E_{pp} corresponding to the ground states (GS) of $^{250-260}\text{No}$ are plotted as functions of the neutron number N . The "average" (AV) E_{pp} values obtained for odd-mass isotopes are also included in the plot.

For example, for ^{252}No and $E_0 = 1.0$ MeV we have obtained $\log_{10} t_{\text{SF}} = 8.7919$ s within the ATD scheme while $\log_{10} t_{\text{SF}} = 6.9928$ s within the GCM one. Another relevant quantity is the parameter E_0 , because increasing it reduces the integration interval in the action and this leads to smaller t_{SF} values in either the ATD or GCM scheme. For example, once more in the case of ^{252}No but with $E_0 = 1.5$ MeV, we have obtained $\log_{10} t_{\text{SF}} = 5.7252$ s and $\log_{10} t_{\text{SF}} = 4.7378$ s within the ATD and GCM approaches, respectively. In the computation of the fission half-lives, the wiggles in the collective masses have been softened by means of a three point filter [19–21].

B. The nucleus ^{253}No

In Fig. 2, we have plotted similar curves as in Fig. 1 but for the fission path of ^{253}No corresponding to the K value of its ground state, i.e., $K_0 = 9/2$. Results corresponding to AV HFB calculations (see, Sec. II) for this odd-mass nucleus have also been included in each panel for the sake of comparison. As can be seen from panel (a) the $K_0 = 9/2$ energy, computed as the HFB-EFA plus the rotational energy, displays as a function of the quadrupole moment, a behavior reminiscent of the one found for ^{252}No . The absolute minimum of the $K_0 = 9/2$ path appears at $Q_{20} = 16$ b and corresponds to a parity-conserving configuration [see, panel (b)] with $\pi = -1$, which agrees well with the experimental [57] $K^\pi = 9/2^-$ ground state for this nucleus. The $9/2^-$ fission iso-

mer at $Q_{20} = 52$ b lies 2.22 MeV above the ground state from which, it is separated by the inner barrier ($Q_{20} = 30$ b) with the height of 11.67 MeV. The left-right symmetry is broken for $Q_{20} \geq 62$ b and the height of the outer barrier ($Q_{20} = 70$ b) turns out to be 5.42 MeV. All these values are obtained with the $K=9/2$ configuration corresponding to the lowest energy for each Q_{20} value of the fission path. In this way, the number just given for the fission isomer might or might not correspond to the lowest energy configuration with the deformation of the fission isomer. In fact, in the case of ^{253}No , the lowest energy configuration at $Q_{20} = 52$ b corresponds to $K=11/2$ and lies at an excitation energy of 2.04 MeV.

On the other hand, the comparison between the EFA and AV paths in panel (a) of Fig. 2, reveals that the former is always higher than the latter and the difference is not constant with the quadrupole moment. The EFA inner and outer barriers (11.67 and 5.42 MeV) are higher than the AV ones (10.91 and 4.62 MeV). The same holds for the EFA (2.22 MeV) and AV (1.63 MeV) excitation energy of the fission isomer. This is a clear manifestation of the specialization energy effect partly due to following the lowest energy configuration with a fixed $K_0 = 9/2$ value.

Note, that the octupole Q_{30} and hexadecupole Q_{40} moments [panel (b)] corresponding to the AV and EFA fission paths follow a rather similar pattern revealing the minute impact of the blocked configuration in the mass moments defining the nuclear shape.

As can be seen from panel (c) of Fig. 2, the HFB-EFA (black dashed line) and AV (red dashed line) proton E_{pp} values can hardly be distinguished. Both the HFB-EFA and AV neutron pairing energies also display a similar pattern. However, the former are much lower than the latter as a consequence of the quenching of pairing correlations due to the unpaired neutron. A direct consequence of this quenching also reflects in the enhancement of the HFB-EFA masses as compared to the AV ones regardless of the ATD and/or GCM scheme used [see, panel (d)]. From Fig. 2, one concludes that the effect of the unpaired neutron is to increase the fission barrier heights and an enhancement of the HFB-EFA collective masses with respect to the AV ones. Both effects go in the direction of increasing the collective action Eq. (11) and therefore, the t_{SF} values Eq. (10) increase in odd-mass nuclei as compared to their even-even neighbors.

Once more, one sees that the ATD masses are larger than the GCM ones leading, for example, to the values $\log_{10} t_{\text{SF}} = 24.5590$ s and $\log_{10} t_{\text{SF}} = 15.3318$ s within the ATD and GCM schemes for ^{253}No and $E_0 = 1.0$ MeV. On the other hand, for $E_0 = 1.5$ MeV we have obtained the values $\log_{10} t_{\text{SF}} = 20.8810$ s and $\log_{10} t_{\text{SF}} = 12.9325$ s within the ATD and GCM approaches, respectively. Due to these differences, and even when there is a lack of detailed theoretical justification for the use of GCM-like masses in the case of odd-mass systems, we have also considered both schemes in the computation of their spontaneous fission half-lives.

C. Systematic of the fission paths in $^{250-260}\text{No}$

In Fig. 3, we have summarized the ground state fission paths obtained for $^{250-260}\text{No}$ as functions of the quadrupole moment Q_{20} . The paths show two minima, the ground state one at $Q_{20} = 16$ b and the fission isomer around $Q_{20} = 52$ b. For all the studied nuclei, our Gogny-D1M calculations predict the super-deformed minimum to be above the normal deformed one though its excitation energy decreases with increasing neutron number [see, panel (b) of Fig. 7]. On the other hand, the top of the inner and outer barriers is located at $Q_{20} \approx 30$ b and $Q_{20} \approx 70$ b, respectively. For all the paths shown in the figure, the outer barriers belong to a parity-breaking sector that decreases their heights as compared with a reflection-symmetric situation. The specialization energy effect becomes apparent from the comparison between the ground state and AV fission paths in the case of odd-mass nuclei.

In good agreement with the experimental data [57], our calculations predict $9/2^-$, $1/2^+$ and $3/2^+$ ground states for ^{253}No , ^{255}No and ^{257}No . This is not the case for the nuclei ^{251}No and ^{259}No where we have obtained $5/2^+$ and $7/2^+$ ground states while the experimental ones correspond to $7/2^+$ and $9/2^+$, respectively. However, for those nuclei we have found $7/2^+$ and $9/2^+$ one-quasiparticle configurations located inside the ground state well whose excitation energies are only 65.55 and 149.62 keV, respectively. Therefore, we have also explored the $K = 7/2$ and $9/2$ fission paths in the case of ^{251}No and ^{259}No . They are plotted in Fig. 4 as functions of Q_{20} . As can be seen, the structure of those paths and the associated specialization energy effect resemble the ones in Fig. 3 (see also, the discussion below).

Using the ground state energies obtained for $^{250-260}\text{No}$, we have computed the one-neutron S_{1N} separation energies shown in Fig. 5. Though our calculations capture the experimental [58] odd-even staggering, the predicted amplitudes are larger than the experimental ones, especially for the heavier isotopes. This could be a consequence of an inappropriate pairing strength in the regions under study or the neglect of many-body effects like particle-vibration coupling or the restoration of the broken $U(1)$ particle number symmetry. Another source of uncertainty is the neglect of time-odd fields in the EFA used in the present calculation that can contribute up to a few hundred keV to the binding energy of odd nuclei [72].

The proton and neutron pairing interaction energies E_{pp} corresponding to the ground states of $^{250-260}\text{No}$ are plotted in Fig. 6 as functions of the neutron number N . The AV E_{pp} values obtained for $^{251,253,255,257,259}\text{No}$ are also included in the plot. For protons the pairing energies exhibit a smooth increase with increasing neutron number. As expected, they are rather similar to the AV ones for $^{251,253,255,257,259}\text{No}$. However, in the case of neutrons, the quenching of the pairing correlations induced by blocking is very severe. We have obtained the ra-

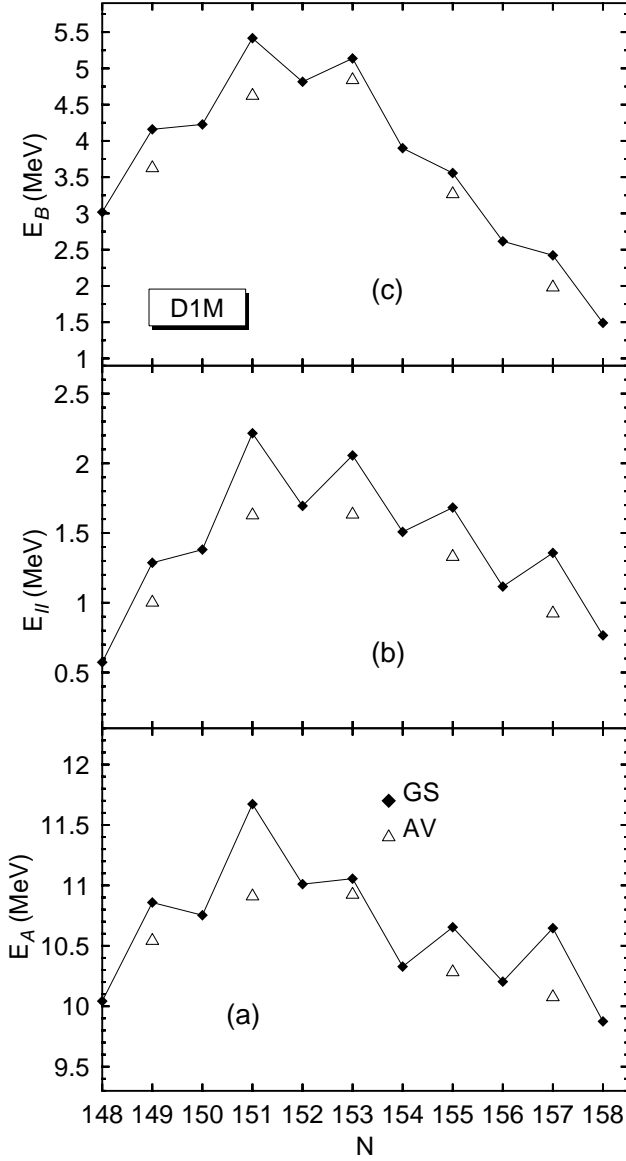


FIG. 7: The inner barrier height E_A , excitation energy of the fission isomer E_{II} and outer barrier height E_B corresponding to the ground state (GS) fission paths shown in Fig. 3 are plotted in panels (a), (b) and (c) as functions of the neutron number. The "average" (AV) values obtained for odd-mass isotopes are also included in the plot.

tios $E_{pp,GS}/E_{pp,AV} = 0.40, 0.21, 0.26, 0.56$ and 0.62 for $^{251,253,255,257,259}\text{No}$. An alternative measure of how effective is the quenching of the neutron pairing correlations is provided by the ratio $\langle \Delta \hat{N}^2 \rangle_{GS} / \langle \Delta \hat{N}^2 \rangle_{AV} = 0.528, 0.08, 0.332, 0.79$ and 0.821 for the same nuclei. For the $K^\pi = 7/2^+ (9/2^+)$ normal deformed minimum in ^{251}No (^{259}No) we have obtained the ratios $E_{pp,GS}/E_{pp,AV} = 0.29 (0.63)$ and $\langle \Delta \hat{N}^2 \rangle_{GS} / \langle \Delta \hat{N}^2 \rangle_{AV} = 0.422 (0.824)$. These results indicate that for the neutron pairing correlations the quenching induced by the self-consistent blocking depends on the considered one-quasiparticle configuration.

TABLE I: The values of $\log_{10} t_{SF}$ (in s) obtained for the $K=7/2$ and $5/2$ fission paths in ^{251}No are given as functions of the parameter E_0 (in MeV). The same quantities are also given for the $K=9/2$ and $7/2$ fission paths in ^{259}No . For details, see the main text.

Nucleus	K	Scheme	E_0			
			0.5 MeV	1.0 MeV	1.5 MeV	2.0 MeV
^{251}No	7/2	GCM	11.3558	8.7824	6.2380	3.5589
^{251}No	7/2	ATD	19.9848	16.0185	11.3774	7.0114
^{251}No	5/2	GCM	11.7274	8.8949	6.1555	3.4046
^{251}No	5/2	ATD	20.3827	16.2834	11.6087	7.3890
^{259}No	9/2	GCM	13.2903	10.6305	7.9765	5.3722
^{259}No	9/2	ATD	22.9660	18.8139	14.2703	8.0629
^{259}No	7/2	GCM	14.1852	11.3998	8.5118	5.1894
^{259}No	7/2	ATD	23.7159	19.1671	13.8127	8.0677

They also show that, at least for some of the studied odd-mass isotopes (for example, ^{253}No) one is dealing with a weak pairing regime. Therefore, a more realistic account of the fission process in those systems would require a dynamical description of the neutron pairing correlations as well as their coupling to the relevant deformation parameters [31].

The inner barrier heights E_A , excitation energies of the fission isomers E_{II} and outer barrier heights E_B corresponding to the ground state fission paths shown in Fig. 3 are displayed in panels (a), (b) and (c) of Fig. 7 as functions of the neutron number N . The corresponding AV quantities for $^{251,253,255,257,259}\text{No}$ are also depicted. The three quantities exhibit pronounced odd-even as well as specialization energy effects. In our calculations the largest E_A , E_{II} and E_B values are obtained for the nucleus ^{253}No ($N = 151$). Moreover, for the $K = 7/2 (9/2)$ fission path in ^{251}No (^{259}No) we have obtained $E_A = 10.88 (10.54)$ MeV, $E_{II} = 1.28 (1.86)$ MeV and $E_B = 3.83 (2.46)$ MeV. These values should be compared with the ones [i.e., $10.86 (10.65)$ MeV, $1.29 (1.36)$ MeV and $4.16 (2.42)$ MeV] shown in the figure which correspond to the ground state paths predicted for those nuclei. Let us mention, that we are aware of the reduction, by a few MeV, of the inner barrier heights once triaxiality is taken into account [19]. In the case of odd-mass nuclei, the polarization effects induced by the unpaired nucleon might also lead to triaxial solutions. Though we have kept axial symmetry along the fission paths of the studied No isotopes, we have also corroborated the already mentioned reduction in the case of the even-even nuclei ^{254}No and ^{256}No . However, as such a reduction comes together with an increase in the collective inertia [36, 73] that tends to compensate in the final value of the action, the role of triaxiality is very limited and has not been taken into account in the computation of the corresponding t_{SF} values.

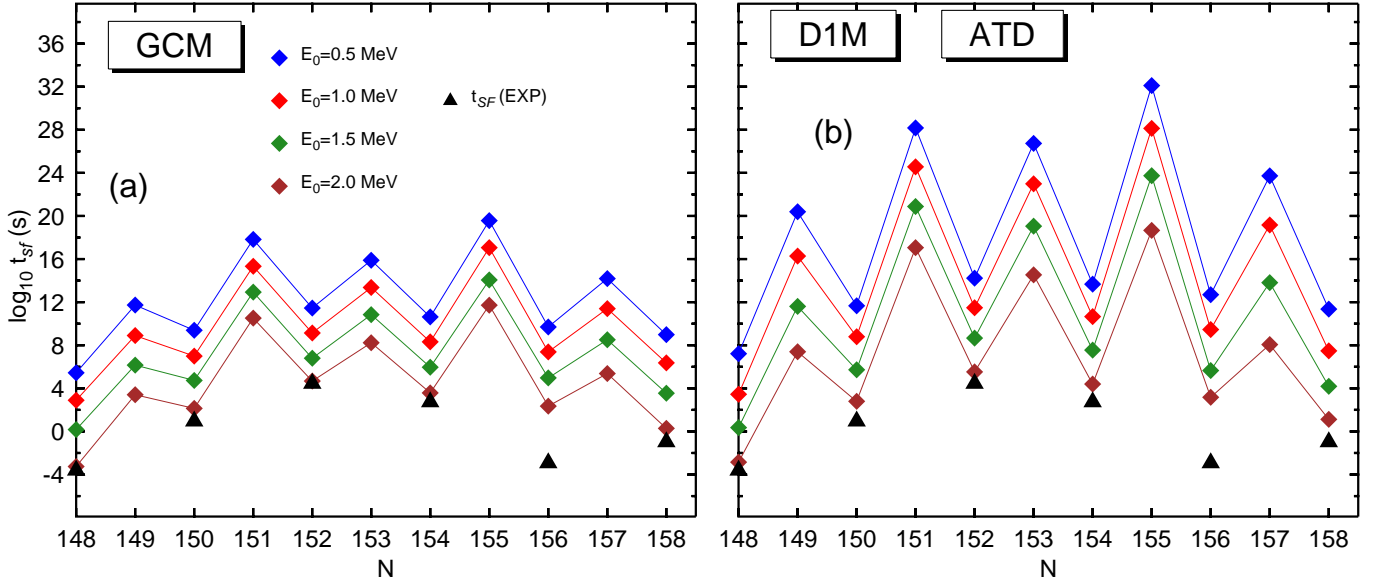


FIG. 8: (Color online) The spontaneous fission half-lives t_{SF} , predicted within the GCM [panel (a)] and ATD [panel (b)] schemes, for the isotopes $^{250-260}\text{No}$ are depicted as functions of the neutron number N . For each isotope, calculations have been carried out with $E_0 = 0.5, 1.0, 1.5$ and 2.0 MeV. The experimental t_{SF} values for even-even isotopes are taken from [14]. For more details, see the main text.

D. Systematic of the spontaneous fission half-lives in $^{250-260}\text{No}$

The ground state spontaneous fission half-lives t_{SF} , obtained within the GCM and ATD schemes, for the isotopes $^{250-260}\text{No}$ are depicted, as functions of the neutron number N , in panels (a) and (b) of Fig. 8, respectively. In the panels we have included the available experimental data for even-even No isotopes [14]. Those data are more scarce for odd-mass nuclei for which only some recommended lower bound values ($t_{SF} \geq 10$ s for ^{251}No , $t_{SF} \geq 28$ min for ^{257}No and $t_{SF} > 10$ h for ^{259}No) can be found in the literature [14]. However, in spite of being only lower bounds, those data already reveal an increase in the spontaneous fission half-lives of the odd-mass isotopes. In our calculations, for each of the studied isotopes, we have considered four values of E_0 (i.e., $E_0 = 0.5, 1.0, 1.5$ and 2.0 MeV). As can be seen from the figure, increasing this parameter leads to a decrease in the predicted spontaneous fission half-lives as well as to an improvement (exception made of ^{258}No) of the agreement with the experiment in the case of even-even nuclei. The predicted ATD t_{SF} values tend to be larger than the GCM ones, with the differences being more pronounced in the case of odd-mass nuclei. For example, for ^{254}No (^{257}No) and $E_0 = 1.0$ MeV we have obtained $\log_{10} t_{SF} = 9.1373$ s ($\log_{10} t_{SF} = 17.0551$ s) within the GCM scheme while the corresponding value within the ATD approach is $\log_{10} t_{SF} = 11.4739$ s ($\log_{10} t_{SF} = 28.1227$ s) [see also, Table I]. Though there exists a strong variance of the theoretical fission rates with respect to the details involved in their computation, the

same trend is always observed, i.e., regardless of the employed scheme and/or E_0 value the fission half-lives exhibit a pronounced odd-even staggering. The amplitude of the staggering (i.e., the difference between the spontaneous fission lifetime of an odd-mass isotope and the one obtained by averaging the values of the two neighboring isotopes) is rather insensitive to the E_0 value considered but it depends strongly both on neutron number and on the kind of collective inertia considered. The amplitude varies from the four orders of magnitude observed for the $N=149$ and $N=157$ isotopes in the calculation with the GCM inertias to the 16 orders of magnitude for the No isotope with $N=155$ in the ATD calculation. The amplitude of the staggering is larger in the ATD than in the GCM case (up to a factor 1.6) as can be expected from the values of the corresponding inertias. The dependence with neutron number shows a seesaw pattern with large values at $N=151$ and $N=155$. On the other hand, the amplitude of the staggering seems to be an interesting quantity to be compared with experimental data given its insensitivity to the E_0 values. Similar features to the ones just discussed also emerge by comparing the spontaneous fission half-lives, given in Table I, for the $5/2$ and $7/2$ fission paths in ^{251}No as well as the $9/2$ and $7/2$ ones in ^{259}No (see, Figs. 3 and 4).

In Fig. 9, we have plotted the α -decay half-lives computed with a parametrization [74] of the Viola-Seaborg formula [75]. To this end, we have used the binding energies obtained for the corresponding nobelium and fermium isotopes. The α -decay half-lives obtained in our Gogny-D1M calculations compare well with the experimental ones [58] as could be expected from the good

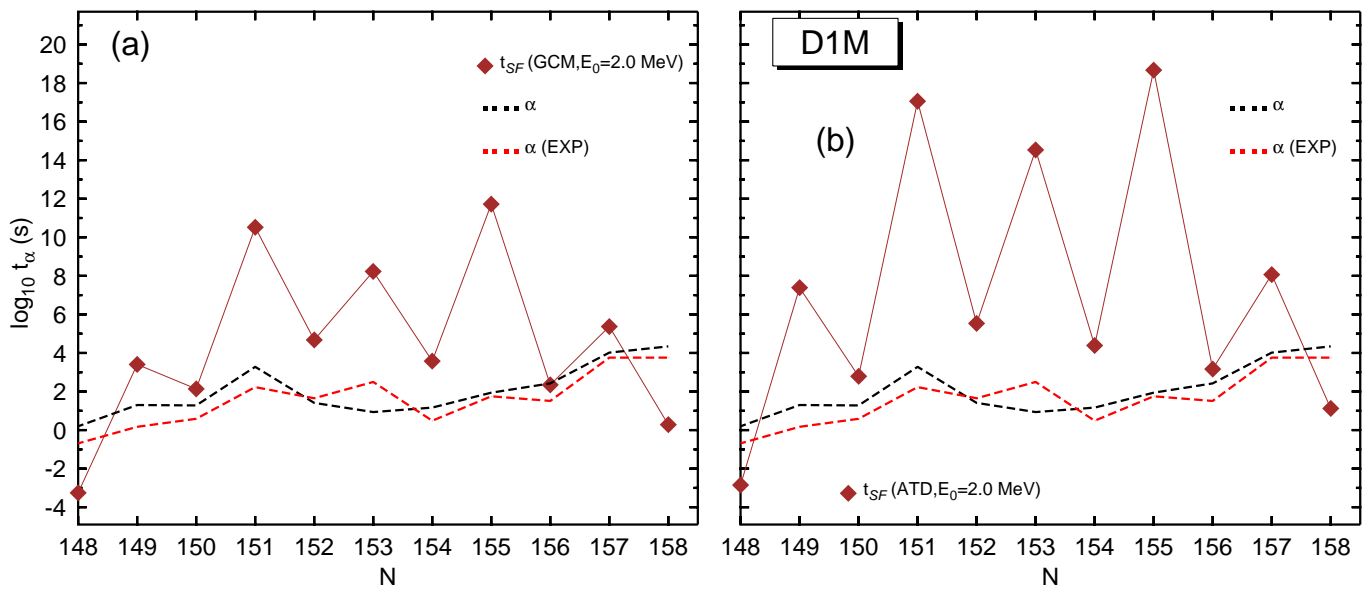


FIG. 9: (Color online) The theoretical and experimental [58] α -decay half-lives are plotted as functions of the neutron number N . They are compared in panel (a) [panel (b)] with the spontaneous fission half-lives obtained within the GCM (ATD) scheme with $E_0 = 2.0$ MeV. For more details, see the main text.

performance of the Gogny-D1M EDF in reproducing experimental binding energies and therefore in reproducing the Q_α values entering the Viola-Seaborg formula. In panel (a), we have also included the spontaneous fission half-lives predicted within the GCM scheme ($E_0 = 2.0$ MeV). From the comparison between the t_α and GCM t_{SF} values we conclude that α -decay is the dominant decay channel for the odd-mass No isotopes considered even for ^{259}No that lies in between two even-even nuclei where spontaneous fission dominates. The same conclusion can be obtained from the comparison with the corresponding ATD fission lifetimes in panel (b).

IV. CONCLUSIONS

In this paper, we have considered the fission properties of a set of nobelium isotopes including even-even and odd-mass nuclei. The selected set comprises $^{250-260}\text{No}$ as a representative sample. We have resorted to the constrained Gogny-D1M mean-field approximation as our main theoretical tool. In particular, the even-even systems have been studied within the standard HFB framework while for the odd-mass isotopes we have used the HFB-EFA in order to reduce the already substantial computational effort. Besides the proton \hat{Z} and neutron \hat{N} number operators, we have employed constraints on the axially symmetric quadrupole \hat{Q}_{20} , octupole \hat{Q}_{30} and \hat{Q}_{10} operators. We have presented a detailed description of the (blocking) methodology used to obtain the (least energy) fission paths in the studied odd-mass isotopes while for the even-even ones calculations have been carried out along the lines discussed in previous

fission studies [19–21]. Zero-point rotational and vibrational corrections have always been added to the HFB and/or HFB-EFA energies *a posteriori*. The rotational correction has been found in terms of the Yoccoz moment of inertia while both the GCM and ATD schemes have been used to compute the collective masses and vibrational corrections. All the required mean-field building blocks have then been used to compute the GCM and/or ATD ground state spontaneous fission half-lives t_{SF} for $^{250-260}\text{No}$ within the WKB formalism. The α -decay half-lives t_α have been found, using the binding energies obtained for the corresponding No and Fm nuclei, with the help of a parametrization of the Viola-Seaborg formula.

For both even-even and odd-mass No isotopes our Gogny-D1M calculations provide ground state fission paths with normal deformed and isomeric minima as well as inner and outer barriers whose quadrupole deformations, remain almost constant as functions of the neutron number. In all cases, the outer barriers belong to a parity-breaking sector that decreases their heights as compared to a reflection-symmetric situation. The inner and outer barrier heights as well as the isomer excitation energies display pronounced odd-even effects as functions of the neutron number with maxima at $N=151$. As a result of following configurations with a fixed K_0 quantum number, the ground state fission paths obtained for the odd-mass nuclei are always higher than the AV ones. This specialization energy effect together with the pronounced quenching of neutron pairing correlations (leading to an enhancement of the GCM and/or ATD collective masses as compared to the AV ones) are fully taken into account via the Ritz-variational minimization of the HFB-EFA energies.

The present calculations represent a first step towards a better understanding of the physics of spontaneous fission in odd-mass nuclei and there is still room for further improvements. For example, the evaluation of the collective inertias relies on approximations that are not fully understood in the finite temperature case which is used to justify the formulas within our EFA methodology. This lack of full understanding leads to phenomenological prescriptions like the one used here to avoid potential divergences when two-quasiparticle energies cross. Another relevant aspect is the kind of treatment used to find the fission path: a dynamical treatment favors stronger pairing correlations than the least energy one employed in the present study and this could substantially change not only the specialization energy but also the collective

inertias. Finally, the lowering of the first barrier due to triaxiality and its impact on the spontaneous fission lifetime in the case of odd-nuclei has still to be elucidated. There is no doubt that all these, still unresolved, aspects of the spontaneous fission in odd-mass nuclei deserve further studies in the future. Work along these lines is in progress and will be reported elsewhere.

Acknowledgments

The work of LMR was supported by the Spanish grants FIS2012-34479-P MINECO, FPA2015-65929-P MINECO and FIS2015-63770-P MINECO.

-
- [1] I. Hamamoto, Phys. Rev. C **79** 014307 (2009).
 - [2] S. Perez-Martin and L.M. Robledo, Phys. Rev. C **78**, 014304 (2008).
 - [3] L. Bonneau, P. Quentin and P. Möller, Phys. Rev. C **76**, 024320 (2007).
 - [4] T. Duguet, P. Bonche, P. -H. Heenen, and J. Meyer, Phys. Rev. C **65**, 014310 (2001).
 - [5] R. Rodríguez-Guzmán, P. Sarriguren, L.M. Robledo, and S. Perez-Martin, Phys. Lett. B **691**, 202 (2010).
 - [6] R. Rodríguez-Guzmán, P. Sarriguren and L.M. Robledo, Phys. Rev. C **82**, 044318 (2010).
 - [7] R. Rodríguez-Guzmán, P. Sarriguren and L.M. Robledo, Phys. Rev. C **82**, 061302(R) (2010).
 - [8] R. Rodríguez-Guzmán, P. Sarriguren and L.M. Robledo, Phys. Rev. C **83**, 044307 (2011).
 - [9] N. Schunck, J. Dobaczewski, J. McDonnell, J. Moré, W. Nazarewicz, J. Sarich and M. Stoitsov, Phys. Rev. C **81**, 024316 (2010).
 - [10] P. Olbratowski, J. Dobaczewski, J. Dudek, and W. Plóciennik, Phys. Rev. Lett. **93**, 052501 (2004).
 - [11] J. Dobaczewski, A.V. Afanasjev, M. Bender, L.M. Robledo, and Y. Shi, Nucl. Phys. A **944**, 388 (2015).
 - [12] S. Björnholm and J.E. Lynn, Rev. Mod. Phys. **52**, 725 (1980).
 - [13] H.J. Specht, Rev. Mod. Phys. **46**, 773 (1974).
 - [14] N. E. Holden and D. C. Hoffman, Pure Appl. Chem. **72**, 1525 (2000).
 - [15] P. Fong, Phys. Rev. C **122**, 1545 (1961).
 - [16] S. A. Giuliani and L.M. Robledo, Phys. Rev. C **88**, 054325 (2013).
 - [17] M. Brack, J. Damgaard, A.S. Jensen, H.C. Pauli, V.M. Strutinsky and C.Y. Wong, Rev. Mod. Phys. **44**, 320 (1972).
 - [18] G.F. Bertsch and H. Flocard, Phys. Rev. C **43**, 2200 (1991).
 - [19] R. Rodríguez-Guzmán and L.M. Robledo, Phys. Rev. C **89**, 054310 (2014).
 - [20] R. Rodríguez-Guzmán and L.M. Robledo, Eur. Phys. J. A **50**, 142 (2014).
 - [21] R. Rodríguez-Guzmán and L.M. Robledo, Eur. Phys. J. A **52**, 12 (2016).
 - [22] H.J. Krappe and K. Pomorski, *Theory of Nuclear Fission*, Lectures Notes in Physics, **838** (Springer, Berlin, 2012).
 - [23] A. Baran, M. Kowal, P. -G. Reinhard, L. M. Robledo, A. Staszczak, and M. Warda, Nucl. Phys. A **994**, 442 (2015).
 - [24] N. Schunck and L.M. Robledo, Rep. Prog. Phys. **79**, 116301 (2016).
 - [25] J. F. Berger, M. Girod, and D. Gogny, Nucl. Phys. A **428**, 23c (1984).
 - [26] J.-P. Delaroche, M. Girod, H. Goutte and J. Libert, Nucl. Phys. A **771**, 103 (2006).
 - [27] N. Dubray, H. Goutte and J.-P. Delaroche, Phys. Rev. C **77**, 014310 (2008).
 - [28] W. Younes and D. Gogny, Phys. Rev. C **80**, 054313 (2009).
 - [29] M. Warda, J. L. Egido, L.M. Robledo and K. Pomorski, Phys. Rev. C **66**, 014310 (2002).
 - [30] M. Warda and J.L. Egido, Phys. Rev. C **86**, 014322 (2012).
 - [31] S. A. Giuliani, L.M. Robledo and R. Rodríguez-Guzmán, Phys. Rev. C **90**, 054311 (2014).
 - [32] N. Nikolov, N. Schunck, W. Nazarewicz, M. Bender and J. Pei, Phys. Rev. C **83**, 034305 (2011).
 - [33] J.D. McDonnell, W. Nazarewicz and J.A. Sheikh, Phys. Rev. C **87**, 054327 (2013).
 - [34] J. Erler, K. Langanke, H.P. Loens, G. Martínez-Pinedo and P.-G. Reinhard, Phys. Rev. C **85**, 025802 (2012).
 - [35] A. Staszczak, A. Baran, W. Nazarewicz, Physical Review C **87**, 024320 (2013).
 - [36] A. Baran, K. Pomorski, A. Lukasiak and A. Sobiczewski, Nucl. Phys. A **361**, 83 (1981).
 - [37] M. Baldo, L.M. Robledo, P. Schuck and X. Viñas, Phys. Rev. C **87**, 064305 (2013).
 - [38] H. Abusara, A.V. Afanasjev and P. Ring, Phys. Rev. C **82**, 044303 (2010).
 - [39] H. Abusara, A.V. Afanasjev and P. Ring, Phys. Rev. C **85**, 024314 (2012).
 - [40] B.-N. Lu, E.-G. Zhao and S.-G. Zhou, Phys. Rev. C **85**, 011301 (2012).
 - [41] S. Karatzikos, A. V. Afanasjev, G. A. Lalazissis and P. Ring, Phys. Lett. B **689**, 72 (2010).
 - [42] A. V. Afanasjev and O. Abdurazakov, Phys. Rev. C **88**, 014320 (2013).
 - [43] P. Ring and P. Schuck, *The Nuclear Many-Body Problem*

- (Springer, Berlin, 1980).
- [44] J. Dechargé and D. Gogny, Phys. Rev. C **21**, 1568 (1980).
 - [45] M. Baranger and M. Veneroni, Ann. Phys. **114**, 123 (1978).
 - [46] H.M. Sommermann, Ann. Phys. **151**, 163 (1983).
 - [47] P. Ring, L.M. Robledo, J.L. Egido, and M. Faber, Nucl. Phys. A **419**, 261 (1984).
 - [48] R. Julin, Nucl. Phys. A **834**, 15c (2010).
 - [49] R.-D. Herzberg and P.T. Greenlees, Prog. Part. Nucl. Phys. **61**, 674 (2008).
 - [50] S. Goriely, S. Hilaire, M. Girod, and S. Péru, Phys. Rev. Lett. **102**, 242501 (2009).
 - [51] J. Dechargé and D. Gogny, Phys. Rev. C **21**, 1568 (1980).
 - [52] F. Chappert, M. Girod, and S. Hilaire, Phys. Lett. B **668**, 420 (2008).
 - [53] R. Rodríguez-Guzmán, L.M. Robledo, and P. Sarriguren, Phys. Rev. C **86**, 034336 (2012).
 - [54] L.M. Robledo and R. Rodríguez-Guzmán, J. Phys. G: Nucl. Part. Phys. **39**, 105103 (2012).
 - [55] R. Rodríguez-Guzmán, L.M. Robledo, P. Sarriguren, and J. E. García-Ramos, Phys. Rev. C **81**, 024310 (2010).
 - [56] L.M. Robledo, R. Rodríguez-Guzmán, and P. Sarriguren, J. Phys. G: Nucl. Part. Phys. **36**, 115104 (2009).
 - [57] E. Browne and J. Tuli, Nuclear Data Sheets **114**, 1041 (2013).
 - [58] G. Audi, A.H. Wapstra and C. Thibault, Nucl. Phys. A **729**, 337 (2003).
 - [59] M. Gaudin, Nucl. Phys. **15**, 89 (1960).
 - [60] S. Perez-Martin and L.M. Robledo, Phys. Rev. C **76**, 064314 (2007).
 - [61] L.M. Robledo and G. F. Bertsch, Phys. Rev. C **84**, 014312 (2011).
 - [62] R. Rodríguez-Guzmán, J.L. Egido and L.M. Robledo, Phys. Lett. B **474**, 15 (2000).
 - [63] R. Rodríguez-Guzmán, J.L. Egido, and L.M. Robledo, Phys. Rev. C **62**, 054308 (2000).
 - [64] J.L. Egido and L.M. Robledo, Lectures Notes in Physics **641**, 269 (2004).
 - [65] M. Girod and B. Grammaticos, Nucl. Phys. A **330**, 40 (1979).
 - [66] M.J. Giannoni and P. Quentin, Phys. Rev. C **21**, 2060 (1980).
 - [67] M.J. Giannoni and P. Quentin, Phys. Rev. C **21**, 2076 (1980).
 - [68] J. Libert, M. Girod and J.P. Delaroche, Phys. Rev. C **60**, 054301 (1999).
 - [69] A. Baran, J. A. Sheikh, J. Dobaczewski, W. Nazarewicz and A. Staszczak, Phys. Rev. C **84**, 054321 (2011).
 - [70] J.L. Egido, D. Dorso, J.O. Rasmussen and P. Ring, Phys. Lett. B **178**, 139 (1986).
 - [71] A. Baran, Phys. Lett. B **76**, 8 (1978).
 - [72] L.M. Robledo, R. Bernard, and G.F. Bertsch, Phys. Rev. C **86**, 064313 (2012).
 - [73] M. Bender, K. Rutz, P.-G. Reinhard, J.A. Maruhn and W. Greiner, Phys. Rev. C **58**, 2126 (1998).
 - [74] T. Dong and Z. Ren, Eur. Phys. J. A **26**, 69 (2005).
 - [75] V.E. Viola Jr. and G.T. Seaborg, J. Inorg. Nucl. Chem. **28**, 741 (1966).